Luminescent solar concentrators with a bottom-mounted photovoltaic cell: performance optimization and power gain analysis

Ningning Zhang (张宁宁)[1], Yi Zhang (张 义)[2], Jun Bao (鲍 骏)[1,3,*], Feng Zhang (张 峰)[1], Sen Yan (闫 森)[1], Song Sun (孙 松)[1], and Chen Gao (高 琛)[1,3,]**

[1]*National Synchrotron Radiation Laboratory, Collaborative Innovation Center of Chemistry for Energy Materials, University of Science and Technology of China, Hefei 230029, China*

[2]*College of Science, Sichuan Agricultural University, Ya'an 625014, China*

[3]*CAS Key Laboratory of Materials for Energy Conversion, Department of Materials Science and Engineering, University of Science and Technology of China, Hefei 230029, China*

**Corresponding author: baoj@ustc.edu.cn; **corresponding author: cgao@ustc.edu.cn*

Received December 31, 2016; accepted February 17, 2017; posted online March 10, 2017

Polymethyl methacrylate (PMMA) plate luminescent solar concentrators with a bottom-mounted (BM-LSCs) photovoltaic (PV) cell are fabricated by using a mixture of Lumogen Red 305 and Yellow 083 fluorescent dyes and a commercial monocrystalline silicon cell. The fabricated LSC with dye concentrations of 40 ppm has the highest power gain of 1.50, which is the highest value reported for the dye-doped PMMA plate LSCs. The power gain of the LSC comes from three parts: the waveguide light, the transmitted light, and the reflected light from a white reflector, and their contributions are analyzed quantitatively. The results suggest that the BM-LSCs have great potential for future low-cost PV devices in building integrated PV applications.

OCIS codes: 350.6050, 040.5350, 220.1770.

doi: 10.3788/COL201715.063501.

Luminescent solar concentrators (LSCs) have been proposed from the 1970s as a potential way of coping with the dwindling fossil fuel and aggravation of environmental problems[1–3]. An LSC with side-mounted solar cells is the most common configuration. The waveguide with a uniformly dispersed luminophore is a core component, which absorbs incident sunlight and re-emits it at a longer wavelength. Trapped in the plate of the LSC via total internal reflection, the re-emitted light is concentrated to small area photovoltaic (PV) cells mounted at the edges of the waveguide[4–6]. It can absorb both direct and diffuse lights without an expensive tracking system, and the cooling systems are also not required because the long-wave radiation can transmit the device[6,7]. More particularly, LSCs have a promising prospect in building integrated PVs (BIPVs) because of their low cost and ability to be made into a variety of shapes[8–12]. In past decades, many efforts have been made to increase the power conversion efficiency (PCE) of the LSCs in different ways. Desmet *et al.*[13] designed a stacked dual waveguide with the size of 5.0 cm × 5.0 cm. The overall efficiency of the LSC was 4.2% based on monocrystalline silicon PVs. Our group fabricated a stable glass laminated LSC using mixture dyes of Red 305 and Yellow 083 as luminescent materials. The highest PCE of 2.28% was achieved with PV cell c overage (the ratio of the area of the PV to the area of waveguide plate) of 11.32%. So far, a record PCE of 7.1% was achieved with four parallel-connected GaAs solar cells coupled to the edges of a bulk-plate LSC (5 cm × 5 cm × 0.5 cm) doped with a mixture of two organic dyes. The luminophore in the waveguide plays a crucial role on the performance of LSCs. Katsagounos *et al.*[14] introduced a kind of europium complexes ($Eu(NO_3)_3(trz\text{-}py)_2 \cdot CH_3CN$) as light concentrators into the LSC, and the photocurrent was increased by a 28% maximum. Li *et al.*[15] reported a new quantum dots (QDs) LSC integrated with heavy metal free $CuInS_2$/ZnS core/shell QDs with a large Stokes shift and high optical efficiency. The as-prepared $CuInS_2$/ZnS QDs possess advantages of a high photoluminescence quantum yield of 81% and a large Stocks shift of more than 150 nm. The PCE of the QDs-LSC-PV device reached more than three folds to that of a pure polymethyl methacrylate (PMMA) -PV device.

Compared to traditional LSCs with the PV cell attached to the edges, the LSCs with a bottom-mounted (BM-LSCs) PV cell, as shown in Fig. 1, are a more effective way for cost reduction and efficiency improvement. In this design, the PV cells can absorb waveguide light and direct transmitted light, contributing to solving the narrow-absorption problem and favoring the reduction of self-absorption due to the shorter transmission distance of fluorescence compared with traditional LSCs[7,16,17]. Recently, the BM-LSCs have been attracted increasing interest. Corrado *et al.*[18] designed and fabricated a kind of thin film BM-LSCs and investigated the influencing factors, including the thickness of the waveguide, edge treatment of the window, cell width, and cell placement. A highest PCE of 6.8% was obtained with PV cell coverage of 31%. Balancing the trade-offs between gain and

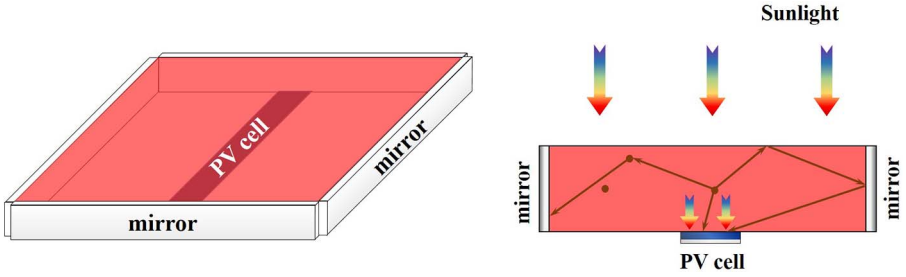

Fig. 1. Schematic of a BM-LSC.

efficiency, the design with the lowest cost per watt attained a power efficiency of 3.8% and a gain of 1.6. Yoon *et al.*[19] designed a type of composite luminescent concentrator PV system that embeds large-scale interconnected arrays of microscale silicon solar cells in thin matrix layers doped with luminophores. The advantage is that the dimensions and designs of the microscale silicon solar cells allowed for the capture of light not only through their top surfaces, but also through their sidewalls and bottom surfaces.

In our previous study, a series of BM-LSCs were fabricated, and the transport process of the waveguide light and the relationship between the BM cells were studied systematically. The LSC device with cell area coverage of 9% achieved a power gain of 1.38[6]. Herein, the PMMA plate-based BM-LSCs with different dye concentration were fabricated. The performance of devices was optimized, and the power gains derived from the contributions of the waveguide light, the transmitted light, and the utilization of a back white reflector were analyzed quantitatively.

The dye-doped PMMA plates were produced by an *in situ* polymerization combing with a casting method. First, the fluorescent dyes Lumogen Red 305 and Yellow 083 (BASF) were mixed with a mass ratio of 2:1, and then dissolved in a methylmethacrylate monomer (MMA, Sinopharm Chemical Reagent Co., Ltd.). The concentrations of the dye mixture in the MMA ranged from 0 to 160 ppm. After a 0.1 wt. % initiator (BPO, Sinopharm Chemical Reagent CO., Ltd.) was added, the mixed solution was heated at 353 K for 1.5 h under continuous stirring. The obtained prepolymer was rapidly poured into a mold consisting of two flat glass plates and a polytetrafluoroethylene gasket. After cooling, cutting, and polishing, the dye-doped PMMA plates with the size of 78 mm × 78 mm × 7 mm were obtained.

The BM-LSCs were fabricated by attaching the commercial monocrystalline silicon PV cell (Trina Solar Co., Ltd., with efficiency around 17.0%, short-circuit current of 204 mA, open-circuit voltage of 0.605 V, and fill factor of 0.752) to the bottom center of the dye-doped PMMA plates using ultraviolet (UV) adhesives (XSSS Optical adhesive UV-3129 with a refractive index of 1.49). The schematic diagram of the fabricated BM-LSC and a photograph of different BM-LSCs with varied dye concentrations ranging from 0 to 160 ppm are shown in Figs. 2(a) and 2(b). Silver mirrors (>85% reflectance for visible light) were attached to the four waveguide edges with UV adhesives.

The absorption and emission spectra of Red 305 and Yellow 083 in ethyl alcohols were measured by a Shimadzu DUV-3700 UV-Visible spectrometer and a Jobin Yvon LUOROLOG-3-TAU spectrometer, respectively. The side emission spectra of the waveguide plates was recorded by an S3000-vis fiber optic spectrometer. The current–voltage (I-V) curves of the fabricated BM-LSC were performed by Keithley 2400 Source Meter under AM 1.5 illumination using an Oriel sol 3 A solar simulator. The power gain is defined as the ratio of the output power of the coupled PV cells to the same bare PV cells,

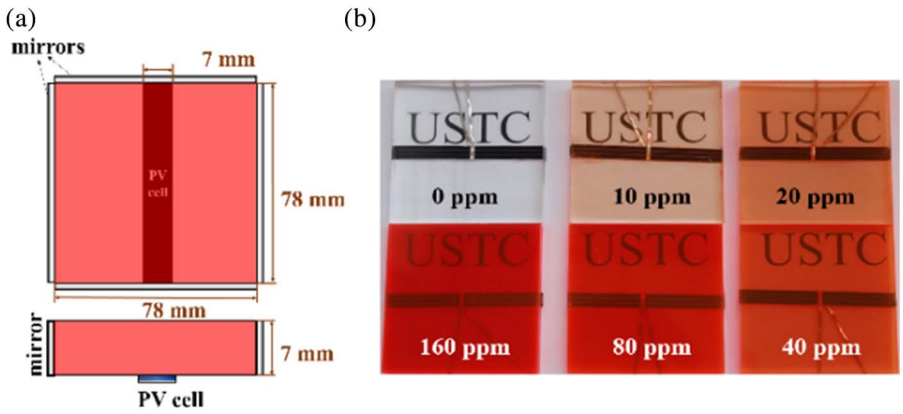

Fig. 2. (a) Schematic diagram of a fabricated BM-LSC. (b) Photograph of the BM-LSCs with varied dye concentrations from 0 to 160 ppm.

$$\text{Gain} = \frac{P_{\max}(\text{LSC})}{P_{\max}(\text{PV})}, \quad (1)$$

where $P_{\max}(\text{LSC})$ and $P_{\max}(\text{PV})$ are the maximum power output of the PV cell attached to BM-LSCs and the same bare PV cells under AM 1.5, respectively.

The fluorescent dyes Lumogen Red 305 and Yellow 083 have the advantages of efficient absorption in the visible light region, good photostability, and high quantum efficiencies (almost 98% for Red 305 and 91% for Yellow 083)[20–22]. Figure 3 shows the absorption and emission spectra of Red 305 and Yellow 083 dissolved in ethyl alcohol solutions, respectively. It can be seen that the Red 305 had a strong absorption in the range of 450–600 nm, covering the low absorption of Yellow 083. Consequently, the mixture of Red 305 and Yellow 083 can enhance the absorption capacity in the visible light region of the solar spectrum as compared to that of the individual dyes. Furthermore, the Red 305 had an emission range of 550–750 nm with a bimodal distribution at 607 and 629 nm, matching well with the absorption of the silicon solar cell.

The doped concentration of mixed dyes in the PMMA plates was optimized according to the measured power gain. A white reflector was added to the bottom side of the LSC (separated by an air gap) to increase the power output, which was made by spraying a cardboard sheet with white paint, as shown in the inset in Fig. 4. From Fig. 4, the doping of the fluorescent dyes mixture increased the power output of the LSC significantly. At the doped concentration of 40 ppm, the power gain of the LSC reached 1.50. To the best of our knowledge, the value is the highest achieved to date for dye-doped PMMA plate LSCs. Further increasing the dye concentration resulted in a slight decrease of power gain.

The self-absorption of dyes refers to the reabsorption of the emitted photons by the emitters[23], thus causing a reduction of the fluorescence signal intensity and

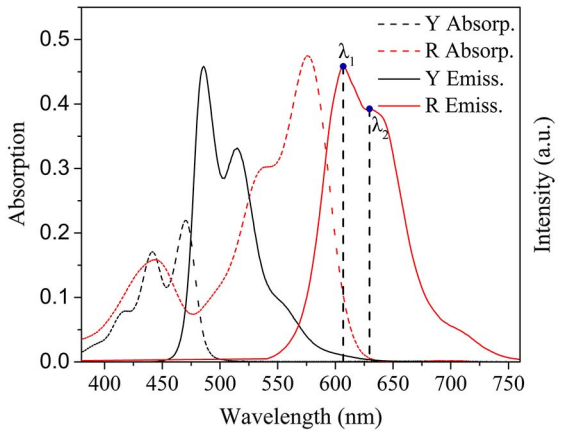

Fig. 3. Normalized absorption (dash line) and emission (solid line) of Yellow 083 (black) and Red 305 (red) in ethyl alcohol. Here, the abbreviations of Y Absorp., R Absorp., Y Emiss., and R Emiss. represent Yellow 083 absorption, Red 305 absorption, Yellow 083 emission, and Red 305 emission, respectively.

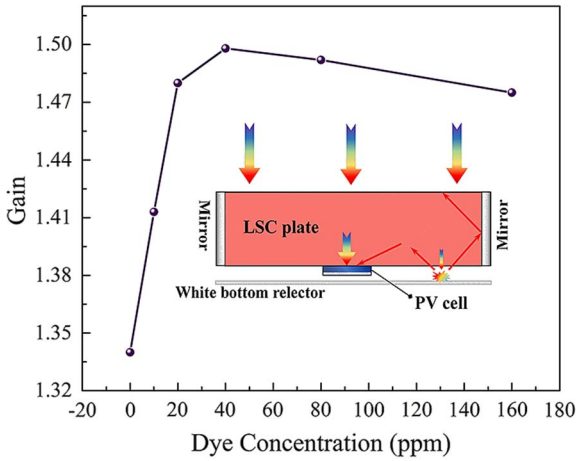

Fig. 4. Gain of BM-LSCs with the enhancement of white back reflector and mirrors as a function of mixed dye concentrations. The inset illustrates the schematic of the light transmission path within a BM-LSC on the white back reflector.

the weakening of the LSC power output[24,25]. The self-absorption of dyes was evaluated qualitatively by measuring the side emission spectra of dye-doped PMMA plates using a fiber optic spectrometer. The schematic diagram of the measurement device is shown in Fig. 5. A laser point (laser lines 405) was used as the excitation light source, illuminating the PMMA plate vertically. A fiber optic probe was fixed on the side of the PMMA plate to detect the emitted waveguide fluorescent light. To avoid the interference of the interface reflected light and external stray light, the side of the PMMA plate except for the measurement zone was blocked using black tape.

Figure 6(a) shows the side emission spectra of the PMMA plate by varying the distance between the laser beam and the fiber optic probe. The dye's concentration in the PMMA plate was 40 ppm. It can be seen that with an increase of distance between the laser beam and fiber probe, the intensity of the emission spectra decreased significantly. In particular, the emission peak at 607 nm

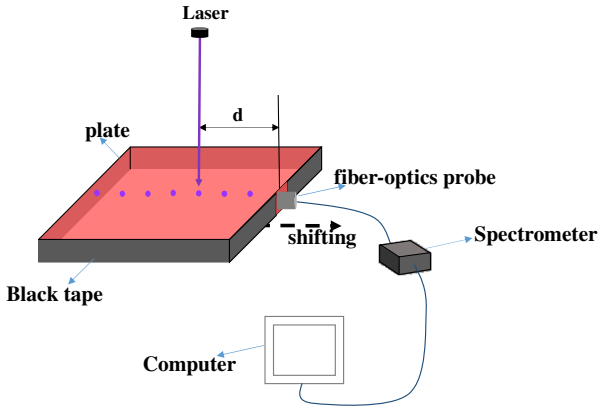

Fig. 5. Schematic diagram of the device for measuring the side emission spectra of dye-doped PMMA plates using a fiber optic spectrometer.

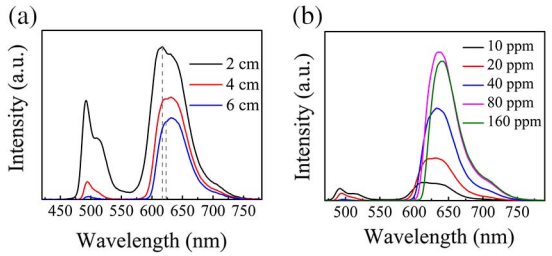

Fig. 6. (a) Side emission spectra of the PMMA plate with the dye concentration of 40 ppm as a function of the distance between the laser beam (405 nm) and fiber probe; (b) the side emission spectra of the PMMA plates with varying dye concentrations. The distance between a 405 nm laser beam and the fiber probe was 4 cm.

decreased more rapidly as compared to that of the peak at 629 nm. The reason was attributed to the emission peak at 607 nm that was overlapped by the absorption range of Red 305, as shown in Fig. 3. The emitted photons were reabsorbed by the dye's molecules during the transmission process, and the degree of self-absorption became larger with the increase of the light transmission distance. The side emission spectra of the PMMA plates with varying dye concentration are shown in Fig. 6(b). With an increase of the dye's concentration, the intensity of the emission spectra increased and reached the highest level at the dye concentration of 80 ppm. Further increasing the dye's concentration resulted in a decrease of the intensity of the emission peak. The reason may be attributed to the higher concentration dyes caused a more serious self-absorption effect.

The BM-LSCs have the advantage of utilizing not only the waveguide light but also the transmitted sunlight and partial fluorescent light in the escape cone, and thus can reduce the cost of PV electricity generation. For the fabricated BM-LSCs shown in the inset in Fig. 4, the total power gain contained three parts to the contributions: the waveguide light, the transmitted light, and the reflected light that goes back to the PMMA plate from the white reflector. To explore the reasons of dependence of power gain on dye concentration, the optical transmission of BM-LSCs was studied through PV characterization, including both transmitted light and waveguide light.

The contribution of transmitted light to the power gain of the LSC was measured using the configuration scheme shown in the inset of Fig. 7. The bare PV cell was placed between the PMMA plate and a black background without optical attachments. The output power was recorded using a Keithley 2400 Source Meter under AM 1.5. In this configuration, the PV cell only absorbed the partial transmitted light (only accounting for about 9% of the total transmitted light), while the rest was absorbed by a black background, and the waveguide light was trapped within the waveguide. Thus, the measured power gain was only attributed to the contribution of the absorbed transmitted light. Figure 7 shows the measured power gain derived from the transmitted light by varying the dye concentration. For

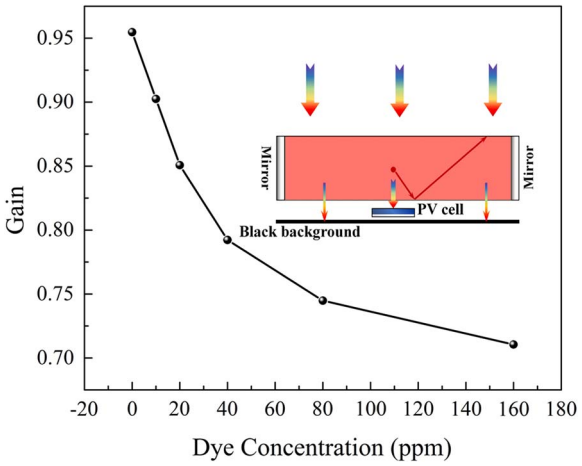

Fig. 7. Power gain derived from the transmitted light with varying dye concentrations. The inset illustrates schematic of measuring the contribution from transmitted light to the BM-LSC power gain.

the undoped transparent PMMA plate, the power gain was 0.95 rather than 1.0. The reason was due to the optical losses mainly caused by the light reflected and absorbed by the PMMA plate. From the Fig. 7, the power gain derived from the transmitted light decreased significantly with an increase of the dye's concentration, which was easy to understand because the doped fluorescent dyes absorbed more incident photons.

The power gain derived from the contribution of waveguide light was measured using the configuration in the inset of Fig. 8. The PV cell was optically attached onto the top of the PMMA plate, and a black background was used. The output power of the attached PV cell was also measured using a Keithley 2400 Source Meter under AM 1.5. In this configuration, the transmitted light was absorbed by the black background rather than reflected back into waveguide plate. Therefore, the PV cell

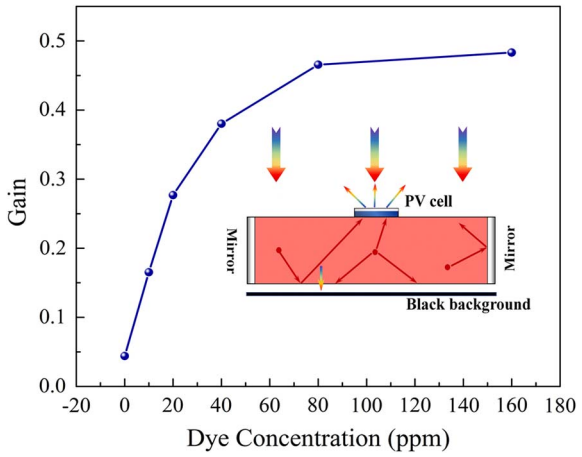

Fig. 8. Power gain derived from the waveguide light with varying dye concentrations. The inset illustrates the schematic of measuring the contribution from waveguide light to the BM-LSC power gain.

only absorbed the waveguide light. Because a portion of incident light was blocked by the reverse side of the attached PV cell, the measured value of output power was calibrated by the ratio of $A_{\text{plate}}/(A_{\text{plate}} - A_{\text{PV}})$, where the A_{plate} and A_{PV} were the areas of the PMMA plate and bare PV cell, respectively. Thus, the power gain of the waveguide light was obtained by the following equation:

$$\text{Gain}_W = P_{\max}(\text{LSC}) \cdot \frac{\left[\frac{A_{\text{plate}}}{A_{\text{plate}} - A_{\text{PV}}}\right]}{P_{\max}(\text{PV})}, \tag{2}$$

where $P_{\max}(\text{LSC})$ and $P_{\max}(\text{PV})$ were the measured maximum power output of the LSC and PV cell, respectively.

The relationship between the gain derived from the waveguide light and dye concentration was presented in Fig. 8. The power gain of the LSC without dyes was approximately 0.04 rather than 0. The doping of the dye increased the output power significantly because the dye enhanced the waveguide emission intensity due to the efficient fluorescence conversion process. When the dye's concentration exceeded 80 ppm, the increase of the gain leveled off, which may be attributed to the serious self-absorption effect.

Table 1 listed the obtained values of power gain derived from the contributions of transmitted light, waveguide light, and reflected light from the back white reflector, respectively, based on the above results. With an increase of the dye's concentration, the contribution of transmitted light to the power gain decreased, while that of the waveguide light increased. The gain derived from the reflected light did not show significant difference by varying the dye's concentration. Comparatively speaking, within the range of dye concentration, the transmitted light contributed most to the output power gain, although only 9% of the transmitted light illuminated the PV cell. Furthermore, the reflected light from the back white reflector also plays an important impact on the output power, its contribution to the total power gain accounted for about 20%. This work analyzed the optical transmission processes of BM-LSCs quantitatively, providing new insight into its power gain mechanism. The results suggest that the BM-LSCs have great potential for future low-cost PV devices in BIPV applications.

Table 1. Power Gain Derived from the Contributions of Transmitted Light, Waveguide Light, and Reflected Light from Back White Reflector

Dye Concentration (ppm)	Gain_W [a]	Gain_t [b]	Gain_r [c]	$\text{Gain}_{\text{total}}$ [d]
0	0.04	0.95	0.34	1.33
10	0.17	0.90	0.35	1.42
20	0.28	0.85	0.35	1.48
40	0.38	0.79	0.33	1.50
80	0.47	0.74	0.28	1.49
160	0.48	0.71	0.28	1.47

[a]Power gain derived from the contribution of waveguide light.
[b]Power gain derived from the contribution of transmitted light.
[c]Power gain derived from the contribution of reflected light from the back white reflector.
[d]Total power gain of the BM-LSCs.

In conclusion, a kind of PMMA plate BM-LSCs is fabricated by using the Lumogen Red 305 and Yellow 083 fluorescent dye and a commercial monocrystalline silicon cell. The power gain of the BM-LSC consists of the contribution of the waveguide light, the transmitted light, and the reflected light that go back to the PMMA plate from the white reflector. When the concentration of dye mixture in the PMMA plate increases from 0 to 160 ppm, the contribution of transmitted light to the power gain decreases, while that of the waveguide light increases. The contribution derived from the reflected light does not show a significant difference. By contrast, the transmitted light contributes the most to the total power gain, although only 9% of the transmitted light illuminates the PV cell. The fabricated BM-LSCs with the dye concentration of 40 ppm have the highest power gain of 1.50, which is the highest value reported to date for dye-doped PMMA plate LSCs.

This work was supported by the National Nature Science Foundation of China (No. U1632273) and the Chinese Academy of Sciences (No. CX3430000001).

References

1. W. H. Weber and J. Lambe, Appl. Opt. **15**, 2299 (1976).
2. W. A. Shurcliff and R. C. Jones, J. Opt. Soc. Am. **39**, 912 (1949).
3. V. Wittwer, W. Stahl, and A. Goetzberger, Sol. Energy Mater. **11**, 187 (1984).
4. X. Long, J. Bai, X. Liu, W. Zhao, and G. Cheng, Chin. Opt. Lett. **11**, 102301 (2013).
5. X. Yu, Y. Gu, D. Chen, X. Zhang, and Y. Liu, Chin. Opt. Lett. **11**, 061301 (2013).
6. Y. Zhang, S. Sun, R. Kang, J. Zhang, N. Zhang, W. Yan, W. Xie, J. Ding, J. Bao, and C. Gao, Energy Convers. Manag. **95**, 187 (2015).
7. J. Zhang, M. Wang, Y. Zhang, H. He, W. Xie, M. Yang, J. Ding, J. Bao, S. Sun, and C. Gao, Sol. Energy **117**, 260 (2015).
8. M. G. Debije and P. P. C. Verbunt, Adv. Energy Mater. **2**, 12 (2012).
9. F. M. Vossen, M. P. J. Aarts, and M. G. Debije, Energy Build. **113**, 123 (2016).
10. B. Norton, P. C. Eames, T. K. Mallick, M. J. Huang, S. J. McCormack, J. D. Mondol, and Y. G. Yohanis, Sol. Energy **85**, 1629 (2011).
11. D. Chemisana, Renewable Sustainable Energy Rev. **15**, 603 (2011).
12. J. W. E. Wiegman and E. van de Kolk, Sol. Energy Mate. Sol. Cells **103**, 41 (2012).
13. B. Rezaie, E. Esmailzadeh, and I. Dincer, Energy Build. **43**, 56 (2011).
14. G. Katsagounos, E. Stathatos, N. B. Abrabatzis, A. D. Keramidas, and P. Lianos, J. Lumin. **131**, 1776 (2011).
15. C. Li, W. Chen, D. Quan, Z. Zhou, J. Qin, Y. Li, Z. He, and K. Wang, Sci. Rep. **5**, 17777 (2015).
16. O. A. Bozdemir, S. Erbas-Cakmak, O. O. Ekiz, A. Dana, and E. U. Akkaya, Angew. Chem. Int. Ed. **50**, 10907 (2011).

17. A. F. Mansour, Polym. Test **22**, 491 (2003).
18. C. Corrado, S. W. Leow, M. Osborn, E. Chan, B. Balaban, and S. A. Carter, Sol. Energ. Mat. Sol. C. **111**, 74 (2013).
19. J. Yoon, L. Li, A. V. Semichaevsky, J. H. Ryu, H. T. Johnson, R. G. Nuzzo, and J. A. Rogers, Nat. Commun. **2**, 343 (2011).
20. W. G. J. H. M. van Sark, K. W. J. Barnham, L. H. Slooff, A. J. Chatten, A. Büchtemann, A. Meyer, S. J. McCormack, R. Koole, D. J. Farrel, R. Bose, E. E. Bende, A. R. Burgers, T. Budel, J. Quilitz, M. Kenndedy, T. Meyer, C. D. M. Donegá, A. Meijerink, and D. Vanmaekelbergh, Opt. Express **16**, 21773 (2008).
21. Y. Zhang, S. Sun, R. Kang, J. Zhang, M. Wang, X. Wei, W. Yan, J. Ding, J. Bao, and C. Gao, Chin. Opt. Lett. **12**, 073501 (2014).
22. T. Dienel, C. Bauer, I. Dolamic, and D. Brühwiler, Sol. Energy **84**, 1366 (2010).
23. G. V. Shcherbatyuk, R. H. Inman, C. Wang, R. Winston, and S. Ghosh, Appl. Phys. Lett. **96**, 191901 (2010).
24. J. S. Batchelder, A. H. Zewail, and T. Cole, Appl. Opt. **18**, 3090 (1979).
25. J. S. Batchelder, A. H. Zewail, and T. Cole, Appl. Opt. **20**, 3733 (1981).